

RSC Advances



This is an *Accepted Manuscript*, which has been through the Royal Society of Chemistry peer review process and has been accepted for publication.

Accepted Manuscripts are published online shortly after acceptance, before technical editing, formatting and proof reading. Using this free service, authors can make their results available to the community, in citable form, before we publish the edited article. This *Accepted Manuscript* will be replaced by the edited, formatted and paginated article as soon as this is available.

You can find more information about *Accepted Manuscripts* in the [Information for Authors](#).

Please note that technical editing may introduce minor changes to the text and/or graphics, which may alter content. The journal's standard [Terms & Conditions](#) and the [Ethical guidelines](#) still apply. In no event shall the Royal Society of Chemistry be held responsible for any errors or omissions in this *Accepted Manuscript* or any consequences arising from the use of any information it contains.

Removal of Malachite Green from Water using Hydrothermally Carbonized Pine Needles

Hassan H. Hammud^{1,2*}, Abeer Shmait², Nadim Hourani³

¹Chemistry Department, Faculty of Science, King Faisal University, Al-Ahsa 31982, Saudi Arabia

²Department of Chemistry, Faculty of Science, Beirut Arab University, Beirut, Lebanon

³Clean Combustion Research Center, King Abdullah University of Science and Technology, Thuwal, Saudi Arabia

Abstract

Hydrothermal carbonization of pine needles (HTC-PN) and its oxidized-activated form HTC-APN are prepared and applied for the adsorption of Malachite Green (MG) in aqueous solution. The HTC materials were characterized by Thermal and TEM analysis. Adsorbent dose, initial concentration of MG, contact time, temperature and pH effect on MG adsorption onto HTC materials were studied. The adsorption equilibrium data was best fitted by Langmuir isotherm model and the adsorption kinetic followed pseudo-second-order model for both HTC-PN and HTC-APN. The maximum capacity predicted by Langmuir nonlinear model is 52.91 and 97.08 mg/g for uptake of MG by HTC-PN and HTC-APN respectively at 30 °C. Thermodynamic investigations showed that the adsorption is spontaneous and endothermic in nature. Results suggest HTC-APN can be used as a low-cost adsorbent for MG removal from industrial wastewater. Yoon-Nelson is the best model with a column capacity of 38.3 mg/g for the adsorption of MG onto HTC-APN.

Keywords: Hydrothermal carbonization, activated, pine needle, adsorption, isotherm, kinetics, column, TEM

1. Introduction

It is estimated that two hundred thousand tones of applied reactive dyes are discharged annually to downstream effluents [1]. In some cases, dye concentration in aqueous effluent can be as high as 800 mg/L [2, 3]. The treatment of effluent containing dyestuff poses considerable problems in the wastewater industry. The removal of dyes from water bodies is extremely important from an environmental point of view [4].

*e-mail: hhammoud@kfu.edu.sa

Malachite green (MG) is classified as cationic dye and is widely used in silk, wool, cotton, leather and paper industries for coloring purposes. MG dye has toxic property which is known to cause carcinogenesis, mutagenesis, and respiratory toxicity [5,6]. Malachite green is not allowed to be used in aquaculture in Mainland, European Union, the United States and Canada. The Panel on Food Safety and Environmental Hygiene (Hong Kong) imposes the prohibition of presence of MG in all food, particularly in fish products [7]. The environmental quality standard limit the concentration of MG in water to 0.5-100 $\mu\text{g/L}$ [8]. Therefore, the removal of MG from wastewater before discharging to the environment is very important.

The present practice for dye removals are aerobic and anaerobic microbial remediation [9, 10], fungal decolorization [11], membrane ultra-filtration [12], reverse osmosis [13], electrochemical treatment [14]. Adsorption has proven to be an efficient method for removal of dyes from wastewater [4,15,16] and it is highly utilized especially if the adsorbent is inexpensive and easily recovered and reused, Gupta et. al [17-21]. A number of adsorbents such as rattan sawdust [5], $\text{Ca}(\text{OH})_2$ treated fly Ash [22], rice husk activated carbon [23], sea shell powder [24] and de-oiled soya [25] have been investigated for the removal of malachite green from water.

Pyrolysis and hydrothermal carbonization are two main processes for production of biochar which can be utilized as adsorbent for the removal of dye from water. Pyrolysis typically utilizes dry biomass for the production of biochar where air pollution is a primary concern due to the emission of volatile compounds. On the other hand, hydrothermal carbonization is an environmentally friendly process which uses water and does not require a totally dry biomass. The final hydro-char product can be easily filtered from reaction mixture. Therefore, hydrothermal carbonization avoids complicated drying schemes, costly separation procedures and pollution problems used in pyrolysis process [26, 27].

The objective of this study was to investigate the feasibility of hydro-char (HTC-PN), prepared by hydrothermal carbonization of pine needles, as an adsorbent for MG removal from water. Additional objectives included activation of hydro-char with H_2O_2 to produce oxidized-activated HTC-APN with additional functional groups, in order to increase the adsorption capacity of cationic dye. The equilibrium and kinetic data of the adsorption processes were then analyzed to study the adsorption isotherm models, kinetics, thermodynamic and mechanism of MG adsorption onto HTC-PN and HTC-APN.

2. Materials and methods

2.1- Materials preparation and characterization

The HTC-PN and HTC-APN biochars were used as adsorbent for removal of Malachite Green (MG) dye (supplied from Aldrich). To prepare hydrothermally carbonized pine needles, 10 g of pine needles and 10 mg of citric acid (as a catalyst for carbonization) in 100 mL of water were subjected to hydrothermal carbonization in a closed vessel for 5 hours at $T_{\max} = 225$ °C. The solid product HTC-PN was then separated from the liquid phase to be used as an adsorbent, 63% yield. To prepare HTC-APN, 3 g of the HTC-PN were immersed in 20 mL of H₂O₂ solution (10%) for 2 h (H₂O₂ was used to oxidize carbonized surfaces and increase oxygen-containing surface functional groups, particularly carboxylic group) [28]. The mixture was then dried in the oven at 80°C for 24 h and the solid obtained (HTC-APN) was washed and dried. HTC-PN and HTC-APN were ground and sieved to less than 0.5 mm to be used for adsorption experiments. De-ionized water was used to prepare the initial standard MG solutions C_0 (25 - 450 ppm) from a stock 1000 ppm MG solution, where ppm = mg/L.

High resolution imaging (*HRTEM*) was performed using a transmission electron microscope operating at 300 kV (Titan Cryo Twin, FEI Company, Hillsboro, OR). Data acquisition was performed using a 4k x 4k CCD camera and an energy filter (US4000, GIF Tridiem, Gatan Inc., Pleasanton, CA).

Thermogravimetric – Differential Thermal Analysis (TG-DTA) curves were recorded on SETARAM LABSYS Thermal analyser in the flow of N₂ within the 25-700°C temperature range, with a heating rate of 3°C/min.

2.2- Adsorption batch study

Adsorption study was carried out in a batch system. In all performed experiments, 250 mL conical flasks each containing malachite green solution of certain concentration and a measured quantity of adsorbent were placed in a shaker incubator with rotation speed of 160 rpm and at constant temperature. At the desired time, the concentration of MG remained in solution was estimated by measuring the absorbance of MG solution at $\lambda_{\max} = 618$ nm with a UV-Vis spectrophotometer (Model: SP-3000 plus, OPTIMA TOKYO- JAPAN) and using calibration curve method.

The % removal of MG from aqueous solution at any time was calculated using eq. (1). The amount of MG adsorbed at equilibrium time, q_e (mg/g), was calculated using eq. (2) and that adsorbed at any time, q_t (mg.g⁻¹), using eq. (3) [29].

$$\% \text{ removal} = \frac{(C_0 - C_t)}{C_0} \times 100 \quad (1)$$

$$q_e = \frac{(C_0 - C_e)V}{m} \quad (2)$$

$$q_t = \frac{(C_0 - C_t)V}{m} \quad (3)$$

where C_0 , C_t and C_e (ppm) are the concentrations of MG in the solution, initially, at any time t and at equilibrium, respectively. V (L) is the volume of the MG solution placed in the flask, and m (g) is the mass of the dry adsorbent used.

To study the effect of HTC-PN dose on MG removal from aqueous solution, experiments were performed at 298 K with 50 mL of MG solution (200 mg/L). The amount of adsorbent added was varied from 0.025 to 0.125 g. Solution pH was kept original without any pH adjustment. Measurements were taken after a contact time of 1 h.

In order to study the effect of initial concentration of MG solution and the contact time on the amount of MG removed from aqueous solution, 100 mL of MG solutions with initial concentrations of 25 - 450 mg/L were placed in a series of flasks. 0.2 g of the adsorbent was then added into each flask and the temperature of the shaker incubator was adjusted to 298 K. In this case, the solution pH was kept original without any adjustment. The amount of MG adsorbed from the solution (50 ppm) was calculated at different times.

The effect of solution temperature on adsorption capacity of the adsorbent was examined by varying the temperature (298, 303, 308, and 313K) of MG solution (50 ppm), by adjusting the temperature controller of the shaker incubator. An adsorbent dose of 2 g/L was used, and solution pH was kept original without any adjustment.

The effect of MG solution pH on adsorption was studied by varying the initial pH from 4 to 10 for a MG initial concentration of 150 mg/L and adsorbent dose of 2 g/L. The pH was adjusted using 0.1 mol/L HCl and/or 0.1 mol/L NaOH and was measured using pH-meter. The temperature controller of the shaker incubator was adjusted to 298 K. Measurements were taken after a contact time of 1 h.

2.3- Isotherm study and adsorption kinetics:

In isotherm experiment, adsorbent dose of 2 g/L was used for MG solutions of different concentrations (25 – 450 mg/L) at different temperatures (298, 303, 308, and 313 K). Malachite green solutions were kept in contact with the adsorbent for 24 hours to ensure that equilibrium is reached for all concentrations studied.

The procedure of kinetic adsorption tests was identical to that of isotherm studies. However, the samples were taken at preset time intervals and constant initial MG dye concentration.

2.4- Column study:

Fixed-bed column study was carried using a column of 2 cm inner diameter, 22 cm height, with bed height of 1.5 cm of HTC-APN (0.5 gm). Malachite green solution of initial concentration 100 mg/L was then added into the column with flow rate of 2 mL/min. The effluent samples were collected at specified intervals of time and were analyzed for the residual MG concentration using UV-Vis spectrophotometer at 618 nm. Column studies were stopped when the column reached exhaustion. After exhaustion, it was necessary to recover MG cations and regenerate the column bed with 1 M HCl solution. The bed was then washed with de-ionized water before being used for another cycle.

2.5- Error analysis

In this study, Chi^2 and SSR were used for the fitting quality of the isotherm and column models to the experimental data.

$$\text{Chi}^2 = \frac{\sum(q_e - q_{e,m})^2}{q_{e,m}} \quad (4)$$

The sum of squared residuals (SSR) measures the total deviation of the calculated values from the fit to the experimental values.

$$\text{SSR} = \sqrt{\frac{\sum(q_e - q_{e,m})^2}{n-1}} \quad (5)$$

Where $q_{e,m}$ (mg/g) is the equilibrium capacity obtained by model's calculation, and q_e (mg/g) is the experimental data of equilibrium capacity, n is the number of data points. If data from the

model are similar to the experimental data, Chi^2 and SSR will be a small number and indicates suitability of the model [30, 31].

3. Results and discussion

3.1- Material characterization:

- HRTEM Analysis

Figure 1 is the HRTEM picture of the local structure of HTC-PN and HTC-APN pine needles. Figure 1 (left) clearly indicates the presence of well ordered array of nanostructure elements in the 20 nm range. Figure 1 (right) indicates the complete change of nanostructure towards a sponge-like cubic mesoporous with a highly functional surface, ideal for water sorption, ion binding, or as a catalyst support, with structural elements also in the 20 nm range.

- Thermal Analysis

The Thermo gravimetric analysis (TGA), derivative thermo gravimetric analysis (dTG), and differential thermal analysis (TG/DTA) of the HTC-PN and HTC-APN samples were undertaken in the range 25 to 700 °C, [32, 33].

For HTC-APN, the TGA and dTG curves shows three mass loss events, Figure 2. The first weight loss corresponds to 6.95 % due to loss of volatile organic compounds in the temperature range 25-150 °C. The second and major weight loss (53.8 %) occurs at 335.2 °C with an associated exothermic heat process ($\Delta H = -288.9$ J/g) and is due to decomposition of organic materials and formation of carbon-carbon bond (carbonization). The third weight loss (21.7 %) in the temperature range 370-600 °C is accompanied with an endothermic heat ($\Delta H = 142.1$ J/g at 554.4 °C) and is related to further HTC-APN degradation as shown by the DTA curve.

For HTC-PN, the TGA, dTG and DTA curves also show a minor weight loss (5.9 %) due to loss of volatile organic compounds. The major weight loss corresponds to 47.7 %. It is accompanied by heat evolution ($\Delta H = -506.3$ J/g) at 305.9 °C due to carbonization effect which occurs at higher extent than that of HTC-APN. Further degradation with a weight loss (20.4 %) occurred in the temperature range 370-600 °C.

3.2- Adsorption study

3.2.1- Effect of adsorbent dose

It was observed that the percent removal of MG (200 mg/L) increased with the adsorbent dose. Increasing the dose of HTC-PN from 0.025 g to 0.125 g results in an increase of percent removal from 1.36 % to 28.05 %. The increase stops for a dose greater than 0.1 g of HTC-PN in 50 mL of MG solution. Thus the optimum dose adopted is 2g/L. Increasing the amount of adsorbent makes a large number of sites available for MG and thus an increase in the extent of adsorption. But overlapping or aggregation of adsorption sites results in a decrease in total adsorbent surface area available to MG and an increase in diffusion path length, and this leads to a slighter increase in MG removal [34,35].

3.2.2- Effect of MG initial concentration and contact time

It was observed that the adsorbed amount of MG increased with the increase in initial solution concentrations (25 - 450 ppm). At low concentration, MG species were located at the outer surface of the hydro-char independently. It can be proposed that an increase in the initial dye concentration leads to an increase in mass gradient between the solution and adsorbent, and this acts as a driving force for the transfer of MG species from bulk solution to the particle size. Results also show that the contact time for 80 % removal of MG from aqueous solution was less than 3 h. This rapid adsorption of MG in the initial stage is due to the abundant availability of active sites on the adsorbent surface. Thereafter, adsorption proceeded at a lower rate due to the fact that the remaining sites were difficult to be occupied [6, 36]. Figure 3 shows the equilibrium % MG removal depending on initial concentration C_i ppm for both HTC-PN and HTC-APN. 92 % and 96 % maximum removal was attained respectively for 25 ppm MG solution and 2g/L adsorbent dose at 30 °C.

3.2.3- Effect of solution temperature

The effect of solution temperature on the adsorption capacity of HTC-PN and HTC-APN for 100 mg/L MG solution was studied. It was observed that the adsorption capacity q_{max} of HTC-PN and HTC-APN increased with solution temperature, which indicates the endothermic nature of the adsorption process, Table 1. This increase in q_{max} is attributed to the sufficient energy

provided by promoted temperature for MG species to reach and adsorb onto hydro-char's interior structure [15].

3.2.4- Effect of pH

The percent removal of MG from aqueous solution increases with increase in solution pH from 4 to 7, then decreases with increase in pH from 7 to 10, Figure SI 1. The highest removal of MG was achieved at pH around 7. At pH values lower than 7 malachite green removal was reduced, possibly as a result of the competition between hydrogen ions and the dye cations for the sorption sites of HTC-PN [36, 37]. At pH values higher than 7, MG removal also decreased due to decrease in electrostatic attraction between MG and HTC-PN (MG is 0 % ionized at pH =10). Thus pH 7 was considered as the optimum pH.

3.3- Adsorption isotherm

Analysis of adsorption isotherm is of fundamental importance to describe how adsorbate molecules interact with the adsorbent surface. The adsorption equilibrium data for HTC-PN and HTC-APN were analyzed using Langmuir and Freundlich isotherm expressions in order to prove the enhancement of adsorption capacity of HTC-APN with respect to HTC-PN. Langmuir isotherm is based on the assumption that the structure of adsorbent is homogeneous, where all adsorption sites are identical and energetically equivalent. That is, each MG/adsorbent process should have equal sorption activation energy and demonstrates the formation of monolayer coverage of dye molecule on the outer surface of the adsorbents. Freundlich isotherm was employed to describe heterogeneous systems and reversible adsorption, which is not restricted to the monolayer formations [38]. The nonlinear forms of Langmuir and Freundlich models [39, 40], are presented in equation 6 and 7 respectively:

$$q_e = \frac{q_{\max} K_L C_e}{1 + K_L C_e} \quad (6)$$

$$q_e = K_f (C_e)^{1/n} \quad (7)$$

The linear form of Langmuir and Freundlich models are presented in equation 8 and 9 respectively:

$$\frac{C_e}{q_e} = \frac{C_e}{q_{\max}} + \frac{1}{K_L q_{\max}} \quad (8)$$

$$\ln q_e = \ln K_F + \frac{1}{n} \ln C_e \quad (9)$$

Where q_e (mg/g) is the experimental amount of MG adsorbed at equilibrium, C_e (mg/L) is the equilibrium concentration of MG in solution, q_{\max} (mg/g) is the Langmuir adsorption capacity of the adsorbent and K_L (L/mg) is Langmuir coefficient related to the affinity between the sorbent and the sorbate. The Freundlich constants K_F (mg/g)(L/mg)^{1/n} and n are indicators of the adsorption capacity and adsorption intensity of the adsorbent. The closer $1/n$ value to 0 the higher heterogeneity in the adsorption [38].

Linear plots of these isotherms (equations 8 and 9) provide the best way to check the best adsorption model fitting to the experimental data and report the adsorption parameters.

Langmuir isotherm appears to be better-fitting than Freundlich model at 30 °C, Figure SI 2, and 3, because it has higher correlation coefficient R^2 value and smaller SSR and Chi^2 values as shown in Table 2. The agreement of experimental data with Langmuir isotherm suggests that the adsorbed MG cations form a monolayer coverage on the HTC-PN surface and on the HTC-APN surface. Results also show that activation of HTC-PN leads to an increase of 83.5 % in q_{\max} value at 30°C obtained from isotherm fitting of data with initial MG concentrations range C_0 (25 - 450 ppm), which means that the activation process has increased the adsorbing power of hydrothermally carbonized pine needles.

The effect of isotherm shape is used to predict the favorability of an adsorption system under specific conditions. The favorable adsorption of Langmuir isotherm can be expressed in terms of a dimensionless constant called equilibrium parameter, R_L , which can be represented as:

$$R_L = \frac{1}{1 + K_L C_0} \quad (10)$$

Where C_0 (mg/L) is the highest initial MG solution concentration studied. R_L value indicates the adsorption nature to be either unfavorable ($R_L > 1$), linear ($R_L = 1$), favorable ($0 < R_L < 1$) or irreversible ($R_L = 0$) [41]. R_L value was 0.028 for HTC-PN and 0.016 for HTC-APN at 303 K for MG solution of initial concentration equal to 200 mg/L. It can be seen that R_L values obtained were between 0 and 1, indicating that the adsorption of MG dye on HTC-PN and on HTC-APN was favorable at the conditions being studied.

3.4- Adsorption kinetic

Adsorption kinetic models (Pseudo-first order and pseudo-second order) were applied to interpret the experimental data to determine the controlling mechanism of dye adsorption from aqueous solution. Experiments were carried out with MG initial concentration of 50 mg/L and adsorbent dose of 2 g/L at four different temperatures.

The linear equation for pseudo-first-order model [42] is:

$$\log(q_{\max} - q_t) = \log q_{\max} - \frac{k_1 t}{2.303} \quad (11)$$

The plot of $\log(q_e - q_t)$ versus t (min) should give a linear relationship from which k_1 and q_{\max} can be determined from the slope and intercept of the plot, respectively. q_{\max} is the predicted maximum capacity mg/L, k_1 (min^{-1}) is the rate constant of pseudo-first-order adsorption. The obtained values of k_1 , q_{\max} and the correlation coefficients R^2 at 303 K are presented in Table 3.

The linear equation for pseudo-second-order model [43] is:

$$\frac{t}{q_t} = \frac{1}{k_2(q_{\max})^2} + \frac{t}{q_{\max}} \quad (12)$$

The plot of t/q_t versus t (min) should give a linear relationship from which q_{\max} and k_2 can be determined from the slope and intercept of the plot, respectively. The values of k_2 , q_e , and R^2 calculated from the plot (Figure 4), are shown in Table 3. Where q_{\max} and q_t are the amount of MG adsorbed at equilibrium and at time t , respectively (mg/g), and k_2 ($\text{g} \cdot \text{mg}^{-1} \cdot \text{min}^{-1}$) is the rate constant of pseudo-second-order adsorption.

Comparing the correlation coefficient values, we find that $R^2 \geq 0.99$ for pseudo-second-order model for HTC-PN and HTC-APN. Besides that, the calculated q_{\max} values obtained for pseudo-second-order model are closer to the experimental $q_{e(\text{exp})}$ values determined from isotherm study than those of pseudo-first-order for HTC-PN and HTC-APN. As a result, the adsorption of MG onto HTC-PN and HTC-APN was found to be fitted well into the pseudo-second-order model.

3.5- Adsorption mechanism

The kinetic results were further analyzed for the adsorption mechanism of HTC-PN and HTC-APN. The most commonly used technique for identifying the mechanism involved in the adsorption process is by fitting the experimental data in an intra-particle diffusion plot [44]. The intra-particle diffusion model [45] can be expressed as:

$$q_t = k_i \cdot t^{1/2} + I \quad (13)$$

where k_i ($\text{mg/g}\cdot\text{min}^{1/2}$) represents the intra-particle diffusion rate constant, and I (mg/g) gives information about the thickness of the boundary layer. Figure SI 4 shows the intra-particle diffusion plots for the adsorption of MG dye on HTC-PN and HTC-APN at 308 K. According to this model, a plot of q_t versus $t^{1/2}$ should be linear if intra-particle diffusion is involved in the adsorption process. If the plot passes through the origin then intra-particle diffusion is the only rate-limiting step. Otherwise, some other mechanisms along with intra-particle diffusion are also involved [6, 46]. As observed, the plot was not linear over the whole time range and can be separated into four linear regions. This may reveal that there are three adsorption stages taking place and a final equilibrium stage:

The initial stage film-diffusion (or chemical reaction) was very fast and this is probably due to a strong electrostatic attraction between MG cations and the external surface of adsorbent.

The liquid film diffusion model is described by equation 14 [47].

$$\ln(1-F) = -k_{fd} \cdot t \quad (14)$$

Where F is the fractional attainment of equilibrium and equal to q_t/q_e , and k_{fd} (min^{-1}) is the film diffusion rate constant. The plots of $\ln(1-F)$ versus t are linear with intercepts I equal to -0.347 and -0.9281 and ($R^2 = 0.9915$ and 0.965) for HTC-PN and HTC-APN respectively. The rate constants k_{fd} , were determined from the slope of the plot (Table 3). The linear plots did not pass through the origin suggesting that the liquid film diffusion model is not the only model to represent adsorption system.

The second and third stages are gradual adsorption stages, where intra-particle diffusion (pore diffusion) are the rate controlling. The two pore diffusion rate constants, k_{i1} and k_{i2} , can be calculated from the slopes of the second and third segments of q vs $t^{1/2}$ plot using equation 13, and they represent the diffusion of MG into pores with two distinct sizes macropores and mesopores respectively (Figure SI 4, Table 3) [5]. The two consecutive linear lines of pore diffusion stages did not pass through the origin. Therefore, intra-particle diffusion was not the only rate limiting step and boundary layer control may be also involved in the process [44]. The value of the intercepts I provides information related to the thickness of the boundary layer. The larger intercepts obtained indicates great contribution of the film surface sorption in the rate-controlling step [6, 48].

The fourth section is final equilibrium stage where intra-particle diffusion started to slow down due to the extremely low adsorbate concentration in the solution or maximum adsorption was attained.

Interaction type between MG and HTC materials

The surface structure of the prepared pine needle hydrochar play a major role in determining the mode of interaction with cationic Malachite Green dye. HTC-PN prepared by hydrothermal carbonization at 225 °C has 1.8 % ash, 52.6 % carbon and a yield of 62.6 %. HRTEM analysis indicates the presence of carbon nanofiber, Figure 1. While Biochar of pine needle from pyrolysis at 250 °C has % ash = 1.2, % C = 61.24 and % yield = 56.1 [49], and biochar of pine needle from pyrolysis at 300 °C has 7.20 % ash, 84.19 % carbon and 57.57 % yield [50].

The interaction of MG and HTC pine needles materials (HTC-PN and HTC-APN materials) are the cooperative effects of four interactions mode:

1) Electrostatic interaction between negative charge of hydrochar HTC material and positive charge of MG dye in analogy with the prediction occurring between negatively charged biochar and cationic methyl violet and rhodanine [51]. This is supported first by the fact that at higher pH where loss of positive charge of MG occurs, the uptake by HTC-PN decreases due to loss of electrostatic attraction. Second, in our study no quantitative uptake of acid orange anion was obtained with HTC materials as a result of repulsion between similar negative charges. 2) π - π electron donor-acceptor interaction between π -electron rich of aromatic graphene in the carbonized region of hydrochar and π -electron deficient of aromatic ring of positively charged Malachite Green [52]. 3) Ion dipole interaction between positive charge of MG and the dipole of polar hydroxyl and carboxylic groups present at the surface of hydrochar. This is supported by our finding that lead cation uptake by HTC-PN and HTC-APN is 41 and 76 mg/g respectively due to favorable complexation with carboxylic and hydroxylic group of HTC materials and consistent with similar studies [28, 53]. The second support is the 83.5 % increase in MG capacity of HTC-APN compared to HTC-PN, as a result of increase in hydroxyl and carboxyl groups in HTC-APN which is prepared by oxidation of HTC-PN with H₂O₂. This result is consistent with previous studies that H₂O₂ treatment can oxidize carbonized surfaces and increase oxygen-containing surface function groups [28].

3.6- Adsorption thermodynamics

- There are three thermodynamic parameters that must be considered to characterize adsorption process which are the enthalpy (ΔH), free energy (ΔG) and entropy (ΔS). The values of ΔH and ΔS can be obtained respectively from the slope and intercept of the Van't Hoff plot of $\ln K_e$ versus $1/T$, Figure SI 5. Where $K_e = C_r / C_e$ is the adsorption equilibrium constant, C_r and C_e (mg/L) are the concentration of MG removed from solution and remained at equilibrium respectively. ΔG is generally calculated from the difference between ΔH and $T \Delta S$ [41,54], Table 1. For HTC-PN and HTC-APN, the positive ΔH values indicate that the adsorption process was endothermic in nature. ΔG values are negative and reflects the spontaneous nature of adsorption process at the range of temperature studied. The decrease in the negative value of ΔG with an increase in temperature indicates that adsorption process is more favorable at higher temperatures. The positive value of ΔS reflects the affinity of the adsorbent towards the adsorbate species.
- In order to evaluate the activation energy of adsorption, Arrhenius equation was applied using the relationship in eq. 15 [54-56]:

$$\ln k = \ln A - E_a / (RT) \quad (15)$$

E_a values can be obtained from the slope of $\ln k_2$ versus $1/T$ plot, Figure SI 6. The magnitude of E_a indicates whether adsorption is mainly physical or chemical in nature. The range of 5-40 kJ/mol of E_a indicates physio-sorption mechanism and the range of 40-800 kJ/mol suggests a chemi-sorption mechanism [46, 56]. The calculated values of E_a for adsorption of MG on HTC-PN and HTC-APN are reported in Table 1. E_a values were more than 40 kJ/mol, indicating that the rate-limiting step in MG adsorption process onto HTC-PN and HTC-APN might be chemically controlled.

The enthalpy of activation (ΔH^\ddagger), entropy of activation (ΔS^\ddagger), and free energy of activation (ΔG^\ddagger) in the adsorption process can be calculated using Eyring equation (eq. 16) [54-56]:

$$\ln \frac{k}{T} = \ln \frac{k_B}{h} + \frac{\Delta S^\ddagger}{R} - \frac{\Delta H^\ddagger}{RT} \quad (16)$$

Where K_B and h are Boltzman and Planck constant respectively. ΔH^\ddagger and ΔS^\ddagger can be determined from the slope and intercept of the plot of $\ln(k/T)$ versus $1/T$, Figure SI 7. The values of ΔH^\ddagger , ΔS^\ddagger and ΔG^\ddagger for adsorption of MG dye onto HTC-PN and HTC-APN are reported in

Table 1. The ΔG^\ddagger values are positive at all temperatures suggesting that adsorption reactions require some energy from an external source to convert reactants into products. A positive value of ΔH^\ddagger implies that the adsorption process is endothermic. A negative value of ΔS^\ddagger suggests that the adsorption process involves an associative mechanism with an increase in order through formation of an activated complex between adsorbate and adsorbent. It also suggests that no significant change occurs in the internal structures of adsorbent during the adsorption process.

3.7- Comparison of capacity of HTC materials with other sorbents

The maximum MG adsorption capacities of various sorbents including HTC materials was compared in Table SI 1, [5, 22-25, 47, 57-62]. The comparison shows that HTC-APN materials has higher adsorption capacity of MG than many other reported adsorbents. The availability of pine needles in nature are some of additional advantages to make these materials ideal for removal of cationic dyes from water. Additional advantage is cost effectiveness since in hydrothermal carbonization of pine needle, the solid phase can be used as adsorbent while the liquid phase containing nutrients can be used for other purposes.

3.8- Column study

A breakthrough curve is a plot of the ratio of C_e/C_0 as a function of time or volume of effluent; where, C_e (mg/L) is the concentration of adsorbate in the effluent, C_0 (mg/L) is the initial concentration of the adsorbate (100 ppm) in the feed solution, and V (mL) is the volume of the effluent collected from the column. The adsorbent dose of HTC-APN was 0.5 g. Figure 5 shows the breakthrough curves for the three cycles of MG adsorption onto HTC-APN in the fixed-bed column. The column capacity obtained from the breakthrough area method [33, 63,64] is 33.9 mg/g, 33.4 mg/g and 32.0 mg/g from the first cycle and the regenerated second and third cycles respectively, with an average of 41.0 % removal. The column saturation of HTC-APN occurred after passage of 450 mL MG solution for the first cycle, and 400 mL for each of the second cycle and third cycle, Figure 5.

The first cycle desorption profile of MG from column bed was plotted (concentration of eluted MG solution vs volume of HCl added), Figure SI 7. The desorption cycle required 305 mL of 1 M HCl solution, with flow rate of 2 mL/min, after which further desorption was negligible. 99.59 % of MG species were desorbed, which shows excellent desorption efficiency.

Three models were used to analyze column performance using the column data for the first cycle of MG adsorption, Figure SI 8. The continuous flow adsorption capacity as well as column kinetic parameters are thus computed. Results are shown in Table 4.

Thomas model is based on the assumption that the process follows Langmuir kinetics of adsorption-desorption. The adsorption model assumes negligible axial dispersion since the rate driving force obeys the second order reversible reaction kinetics.

The non-linear form of Thomas model is:

$$\frac{C_e}{C_0} = \frac{1}{1 + e^{\frac{K_T}{Q}(q_T m - C_0 V)}} \quad (17)$$

Where K_T (mL/mg.min) is Thomas rate constant, q_T (mg/g) is the equilibrium adsorption capacity, m (g) is the amount of adsorbent in the column, Q (mL/min) is the volumetric flow rate, C_0 (mg/L) is the initial concentration of the adsorbate in the feed solution [65, 66].

Yoon-Nelson developed a model based on the assumption that the rate of decrease in the probability of adsorption for each adsorbate molecule is proportional to the probability of adsorbate adsorption and the probability of adsorbate breakthrough on the adsorbent.

The non-linear form of Yoon-Nelson model is:

$$\frac{C_e}{C_0} = \frac{1}{1 + e^{K_{YN}(\tau - t)}} \quad (18)$$

Where K_{YN} (min^{-1}) is the rate constant and τ_{YN} (min) is the time required for 50% adsorbate breakthrough, Figure 6 [67].

The nonlinear form of Yan et al model is:

$$\frac{C_e}{C_0} = 1 - \frac{1}{1 + \left(\frac{Q^2 t}{K_Y q_Y m} \right)^{\frac{K_Y C_0}{Q}}} \quad (19)$$

Where K_Y (L/min.mg) is the kinetic rate constant for Yan et al model, q_Y (mg/g) is the maximum adsorption capacity of adsorbent estimated by Yan model [68].

Comparing the values of Chi^2 , SSR, and R^2 , we find that both the Thomas and Yoon-Nelson models can be used to describe the behavior of the adsorption of MG in a fixed-bed column with a capacity value of 37.9 and 38.8 mg/g respectively. The value of R^2 for Yan et al model was

lower than those for Thomas and Yoon-Nelson models under the same experimental conditions, this makes Yan model less applicable, Table 4 [33].

4. Conclusion

HTC-PN was shown to be a promising adsorbent for removal of MG from aqueous solution over a wide range of concentrations, and the adsorption capacity of HTC-PN was improved by the activation process used in the preparation of HTC-APN reaching a value of 97.1 mg/g. The adsorption of MG was found to increase with increase in contact time, MG initial concentration and solution temperature. Solution pH around 7 proved to be more favorable for adsorption of MG on the HTC-PN and HTC-APN. The Langmuir isotherm model and the pseudo-second order kinetic model were found to fit the adsorption data very well. From the thermodynamic studies, the adsorption process was found to be endothermic and spontaneous in nature. Yoon Nelson proved to be the best model for column adsorption studies, and the capacity for a column packed with HTC-APN is calculated to be 38.3 mg/g.

Acknowledgements

The authors acknowledge research support from Dr. Mani Sarathy of the KAUST Clean Combustion Research Center and Scientists of the KAUST Core Lab Facilities for the TEM analysis (Rachid Sougrat). Youssef fawaz is also thanked for preparation of hydrothermally carbonized (HTC) pine materials.

References

- 1 S. S. Azhar, A. G. Liew, D. Suhardy, K. F. Hafiz, M. D.I Hatim, Dye removal from aqueous solution by using adsorption on treated sugarcane bagasse. *American Journal of applied Sciences*, 2005, 2, 1499-1503.
- 2 Q. H. Hu, S. Z. Qiao, F. Haghseresht, M. A. Wilson, G. Q. Lu, Adsorption study for removal of basic red dye using bentonite. *Industrial and Engineering Chemistry Research*, 2006, 45, 733-738.
- 3 L. P. Linh, U. Eldemerdash, N. Mansor, Y. Uemura, and E. Furuya, Evaluation of adsorptive removal of malachite green from aqueous solutions using *Hevea Brasiliensis*, *International Journal of biomass and renewable*, 2012, 1(2), 32-38.
- 4 V. Vimonses, S. Lei, Bo Jin, C. W. K. Chow, C. Saint, Kinetic study and equilibrium isotherm analysis of Congo Red adsorption by clay materials, *Chemical Engineering Journal*, 2009, 148, 354-364.
- 5 B. H. Hameed, M. I. El-Khaiary, Malachite green adsorption by rattan sawdust: Isotherm, kinetic and mechanism modeling, *J. Hazardous Materials*, 2008, 159, 574–579.
- 6 M. A. Ahmad, R. Alrozi, Removal of malachite green dye from aqueous solution using rambutan peel-based activated carbon: Equilibrium, kinetic and thermodynamic studies, *Chem. Engineering Journal*, 2011, 171, 510– 516.
- 7 D. Wolf, C. Yuen, Food and Agricultural Import Regulations and Standards Subject: Chemicals allowed in Hong Kong Food Regulations, U.S. Consulate General, Hong Kong, (2006) www.fas.usda.gov/gainfiles/200608/146208535.pdf
- 8 Environmental Standards for discharges to surface waters, Supporting Guidance (WAT-SG-53) SEPA Scottish Environment Protection Agency, v.4, 2013 <http://www.sepa.org.uk/water/regulations/guidance>
- 9 A. B. Dos Santos, F. J. Cervantes, J. B. Van Lier, Review paper on current technologies for decolourisation of textile wastewaters: perspectives for anaerobic biotechnology, *Bioresour. Technol.*, 2007, 98, 2369–2385.
- 10 C. T. M. J. Frijters, R. H. Vos, G. Scheffer, R. Mulder, Decolorizing and detoxifying textile wastewater, containing both soluble and insoluble dyes, in a full scale combined anaerobic/aerobic system, *Water Res.*, 2006, 40, 1249–1257.

- 11 Wesenberg D., Kyriakides I., Agathos S.N., White-rot fungi and their enzymes for the treatment of industrial dye effluents, *Biotechnol. Adv.*, 2003, 22, 161–187.
- 12 M. Marcucci, G. Nosenzo, G. Capannelli, I. Ciabatti, D. Corrieri, G. Ciardelli, Treatment and reuse of textile effluents based on new ultrafiltration and other membrane technologies, *Desalination*, 2001, 138, 75–82.
- 13 N. Al-Bastaki, Removal of methyl orange dye and Na_2SO_4 salt from synthetic waste water using reverse osmosis, *Chem. Eng. Process.*, 2004, 43, 1561–1567.
- 14 V. K. Gupta, R. Jain, S. Varshney, Electrochemical removal of the hazardous dye Reactofix Red 3 BFN from industrial effluents, *J. Colloid Interface Sci.*, 2007, 312, 292–296.
- 15 L. Zhengang, F. Zhang, Removal of lead from water using biochars prepared from hydrothermal liquefaction of biomass, *Journal of Hazardous Materials*, 2009, 167, 933–939.
- 16 L. Zhengang, F. Zhang, J. Wu, Characterization and application of chars produced from pinewood pyrolysis and hydrothermal treatment, *Fuel*, 2010, 89, 510–514.
- 17 V. K. Gupta., Application of low-cost adsorbents for dye removal – a review, *J. Environ. Manage.*, 2009, 90, 2313–2342.
- 18 A. Mittal, V. K. Gupta, A. Malviya, J. Mittal, Process development for the batch and bulk removal and recovery of a hazardous, water-soluble azo dye (Metanil Yellow) by adsorption over waste materials (Bottom Ash and De-Oiled Soya), *Journal of Hazardous Materials*, 2008, 151 (2–3), 821–832.
- 19 A. Mittal, J. Mittal, A. Malviya, D. Kaur, V. K. Gupta, Adsorption of hazardous dye crystal violet from wastewater by waste materials, *Journal of Colloid and Interface Science*, 2010, 343(2), 463–473.
- 20 A. Mittal, J. Mittal, A. Malviya, D. Kaur, V. K. Gupta, Decoloration treatment of a hazardous triarylmethane dye, Light Green SF (Yellowish) by waste material adsorbents, *J. Colloid and Interface Science*, 2010, 342 (2), 518–527.
- 21 V. K. Gupta, A. Mittal, D. Jhare, J. Mittal, Batch and bulk removal of hazardous colouring agent Rose Bengal by adsorption techniques using bottom ash as adsorbent, *RSC Advances*, 2012, 2, 8381–8389.

- 22 S. Chowdhury, P. Saha, Adsorption Thermodynamics and Kinetics of Malachite Green onto $\text{Ca}(\text{OH})_2$ Treated Fly Ash, *Journal of Environmental Engineering*, 2011, 137(5), 388-397.
- 23 I. A. Rahman , B. Saad, S. Shaidan, E. S. Sya Rizal, Adsorption characteristics of malachite green on activated carbon derived from rice husks produced by chemical–thermal process *Bioresource Technology*, 2005, 96, 1578–1583.
- 24 S. Chowdhury, P. Saha, Sea shell powder as a new adsorbent to remove Basic Green 4 (Malachite Green) from aqueous solutions: Equilibrium, kinetic and thermodynamic studies, *Chem. Engineering Journal*, 2010, 164, 168–177.
- 25 A. Mittal, L. Krishnan, V. K. Gupta, Removal and recovery of malachite green from wastewater using an agricultural waste material, de-oiled soya, *Separation and Purification Technology*, 2005, 43, 125–133.
- 26 J. W. Lee, *Advanced Biofuels and Bioproducts*, Springer, 2012, 168-169.
- 27 J. A. Libra, K. S. Ro, C. Kammann, A. Funke, N. D. Berge, Y. Neubauer, M. Magdalena Titirici, C. Fühner, O. Bens, J. Kern and Karl-Heinz Emmerich, Hydrothermal carbonization of biomass residuals: a comparative review of the chemistry, processes and applications of wet and dry pyrolysis, *Biofuels*, 2011, 89–124.
- 28 Y. Xue, B. Gao, Y. Yao, M. Inyang, M. Zhang, A. R. Zimmerman, K. S. Ro, Hydrogen peroxide modification enhances the ability of biochar (hydrochar) produced from hydrothermal carbonization of peanut hull to remove aqueous heavy metals: Batch and column tests, *Chemical Engineering Journal*, 2012, 200–202, 673–680.
- 29 M. R. Hadjmohammadi, Mina Salary and Pourya Biparva, Removal of Cr (VI) from aqueous solution using pine needles powder as a biosorbent, *J. Appl. Science*, in *Environmental Sanitation*, 2011, 6, 1-13.
- 30 Y. S. Ho, A. E. Ofomaja, Pseudo-second-order model for lead ion sorption from aqueous solutions onto palm kernel fiber, *Journal of Hazardous Materials*, 2006, B129, 137–142.
- 31 N. Abdel-Jabbar, S. Al-Asheh, Factorial Design for the Analysis of Packed-bed Sorption of Copper using Eggshell as a Biosorbent, *Journal of environmental protection science*, 2009, 3, 133 – 139.

- 32 H. H. Hammud, L. Fayoumi, H. Holail, E-S. M.E. Mostafa, Biosorption studies of methylene blue by Mediterranean algae *Carolina* and its chemically modified forms. Linear and nonlinear models' prediction based on statistical error calculation, *Intern. J. Chem.*, 2011, 3(4), 147-163.
- 33 H. H. Hammud, M. M. Chahine, B. El Hamaoui and Y. Hanifehpour, Lead uptake by new silica-carbon nanoparticles, *European J. of Chem.*, 2013, 4(4), 432-440.
- 34 A. A. Lewinsky, *Hazardous Materials And Wastewater: Treatment, Removal And Analysis*, Nova Publishers (2007) 228, 239, 242, 292.
- 35 M-H. Baek, C. O. Ijagbemi, S-J. O, D-S. Kim, Removal of Malachite Green from aqueous solution using degreased coffee bean, *Journal of Hazardous Materials*, 2010, 176, 820-828.
- 36 F. Deniz, S. Karaman, Removal of Basic Red 46 dye from aqueous solution by pine tree leaves, *Chem. Eng. J.*, 2011, 170, 67-74.
- 37 M. Abedi and Z. Bahreini, Preparation of Carbonaceous Adsorbent from Plant of *Calotropis Gigantea* by Thermo-Chemical Activation Process and its Adsorption Behavior for Removal of Methylene Blue, *World Applied Sciences Journal*, 2010, 263-268.
- 38 H. Gökçekus, *Survival and Sustainability: Environmental Concerns in the 21st Century*, Springer, 2011, 903, 978.
- 39 I. Langmuir, The constitution and fundamental properties of solids and liquids, *J. Am. Chem. Soc.*, 1916, 38 (11), 2221–2295.
- 40 H. M. F. Freundlich, Over the adsorption in solution, *J. Phys. Chem.*, 1906, 57, 385–470.
- 41 *Separation Processes*, Center of Advanced Study. By Banaras Hindu University, Allied Publishers, 2009, 142-144.
- 42 S. Lagergren, About the theory of so-called adsorption of soluble substances, *K.Sven. Vetenskapsakad. Handl.*, 1898, 24 (4), 1–39.
- 43 Y. S. Ho, Adsorption of heavy metals from waste streams by peat, Ph.D. Thesis, University of Birmingham, Birmingham, UK, 1995.
- 44 E. Worch, *Adsorption Technology in Water Treatment: Fundamentals, Processes, and Modeling*, Walter de Gruyter, 2012, 123-124.
- 45 W. J. Weber Jr, J. C. Morriss, Kinetics of adsorption on carbon from solution, *J. Sanit. Eng. Div. Am. Soc. Civ. Eng.*, 1963, 89, 31-60.

- 46 H. K. Boparai, M. Joseph, D. M. O'Carroll, Kinetics and thermodynamics of cadmium ion removal by adsorption onto nano zerovalent iron particles, *Journal of Hazardous materials*, 2011, 186(1), 458-465..
- 47- S. Chowdhury, R. Mishra, P. Saha, P. Kushwaha, Adsorption thermodynamics, kinetics and isosteric heat of adsorption of malachite green onto chemically modified rice husk, *Desalination*, 2011, 265 159–168
- 48 A. Gurses , C. Dogar, M. Yalc, M. A. kyıldız, R. Bayrak, S. Karaca, The adsorption kinetics of the cationic dye, methylene blue, onto clay, *Journal of Hazardous Materials*, 2006, B131 217–228.
- 49 B. Chen, D. Zhou, L. Zhu, Transitional adsorption and partition on nonpolar and polar aromatic contaminants by biochars of pine needles with different pyrolytic temperatures. *Environ. Sci. Technol.* 2008, 42, 5137–5143.
- 50 a) M. Ahmad, S. S. Lee, A. U. Rajapaksha, M. Vithanage, M. Zhang, J. S. Cho, S. E. Lee, Y. S. Ok, Trichloroethylene adsorption by pine needle biochars produced at various pyrolysis temperatures, *Bioresource Technology* 143 (2013) 615–622. b) Ahmad, M., et al. Biochar as a sorbent for contaminant management in soil and water: A review. *Chemosphere* 2013, <http://dx.doi.org/10.1016/j.chemosphere.2013.10.071>.
- 51 R. K. Xu, S.C. Xiao, J. H. Yuan, A. Z. Zhao,. Adsorption of methyl violet from aqueous solutions by the biochars derived from crop residues. *Bioresour. Technol.*, 2011, 102, 10293–10298.
- 52 M. Teixido, J. J. Pignatello, J. L. Beltran, M. Granados, J. Peccia, Speciation of the ionizable antibiotic sulfamethazine on black carbon (biochar). *Environ. Sci. Technol.*, 2011, 45, 10020–10027.
- 53 Z. Liu, F. Zhang, Removal of lead from water using biochars prepared from hydrothermal liquefaction of biomass, *J. Hazard. Mater.*, 2009, 167, 933–939.
- 54 P. Saha, S. Chowdhury, S. Gupta, I. Kumar , Insight into adsorption equilibrium, kinetics and thermodynamics of Malachite Green onto clayey soil of Indian origin *Chem. Eng. Journal*, 2010, 165(3), 874-882
- 55 M.J. Clugston, R. Flemming, *Advanced Chemistry*, Oxford University Press, 2000, 268.
- 56 N. Jiwalak, S. Rattanaphani, J. B. Bremner and V. Rattanaphani, Equilibrium and kinetic modeling of the adsorption of indigo carmine onto silk, *Fibers and Polymers*, 2010, 11 (4), 572-579.

- 57 M. H. Baek, C. O. Ijagbemi, O. Se-Jin, D. S. Kim, Removal of Malachite Green from aqueous solution using degreased coffee bean, *J. Hazard. Mater.* 2010, 176, 820–828.
- 58 K. V. Kumar, S. Sivanesan, Isotherms for Malachite Green onto rubber wood (*Hevea brasiliensis*) sawdust: comparison of linear and non-linear methods, *Dyes Pigments*, 2007, 72, 124–129.
- 59 V. K. Garg, R. Gupta, A. B. Yadav, R. Kumar, Dye removal from aqueous solution by adsorption on treated sawdust, *Bioresour. Technol.*, 2003, 89, 121–124
- 60 C. A. Basar, Applicability of the various adsorption models of three dyes adsorption onto activated carbon prepared apricot, *J. Hazard. Mater.* 2006, B135, 232–241.
- 61 I. D. Mall, V. C. Srivastava, N. K. Agarwal, I. M. Mishra, Adsorptive removal of Malachite Green dye from aqueous solution by bagasse fly ash and activated carbon-kinetic study and equilibrium isotherm analyses, *Colloids Surf. A*, 2005, 264, 17–28.
- 62 R. Malik, D. S. Ramteke, S. R. Wate, Adsorption of malachite green on groundnut shell waste based powdered activated carbon, *Waste Management*, 2007, 27 1129–1138.
- 63 K. H. Chu, , Improved fixed bed models for metal biosorption, *Chemical Engineering Journal*, 2004, 97, 233-239.
- 64 E. Malkoc, Y. Nuhoglu, , Removal of Ni(II) ions from aqueous solutions using waste of tea factory: adsorption on a fixed bed column, *Journal of Hazardous Materials*, 2006, B135, 328-336.
- 65 N. Khan, E. M. Yahaya, I. Abustan, M. F. Pakir, M. Latiff, O. S. Bello, M. A. Ahmad, Fixed-bed column study for Cu (II) removal from aqueous solutions using rice husk based activated carbon, *International Journal of Engineering & Technology*, 2011, 11, 186-190.
- 66 M. Auta, Fixed Bed Adsorption Studies of Rhodamine B Dye using Oil Palm Empty Fruits Bunch Activated Carbon, *Journal of Engineering Research and Studies*, 2012, 3(3) 3-6.
- 67 A. Tarendash, Let's review chemistry, the physical setting, *Barron's Educational Series* 2006.
- 68 F. Zeinali, A. A. Ghoreyshi, Adsorption of Dichloromethane from Aqueous Phase using Granular Activated Carbon: Isotherm and Breakthrough Curve measurements, *Middle-east Journal of scientific Research*, 2010, 5(4), 192-198.

Table 1. Variation of q_{\max} with temperature (Isotherm). Thermodynamics parameters and activation energy for the adsorption of MG onto HTC-PN and HTC-APN for 50 ppm initial MG concentration.

Adsorbent	T (K)	q_{\max} (Langmuir) (mg/g)	K_e ± 0.01	ΔG (kJ/mol) ± 0.05	k_2 (g/mg.min) ± 0.001	ΔG^\ddagger (kJ/mol) ± 0.1
HTC-PN	298	48.78	8.75	-5.47	0.00222	98.99
	303	52.91	11.20	-6.01	0.00327	99.90
	308	55.55	13.82	-6.54	0.00388	100.81
	313	57.14	14.40	-7.08	0.00560	101.72
			ΔH (kJ/mol) ± 0.05	ΔS (J/mol.K) ± 0.1	ΔH^\ddagger (kJ/mol) ± 0.05	ΔS^\ddagger (J/mol.K) ± 0.1
		26.53	107.4	44.60	-182.4	47.01
Adsorbent	T (K)	q_{\max} (Langmuir) (mg/g)	K_e ± 0.01	ΔG (kJ/mol) ± 0.05	k_2 (g/mg.min) ± 0.001	ΔG^\ddagger (kJ/mol) ± 0.1
HTC-APN	298	89.54	51.64	-9.54	0.00407	97.13
	303	97.08	55.04	-10.29	0.00535	97.23
	308	103.09	66.44	-11.04	0.0111	97.34
	313	114.23	103.46	-11.79	0.0238	97.45
			ΔH (kJ/mol) ± 0.05	ΔS (J/mol.K) ± 0.1	ΔH^\ddagger (kJ/mol) ± 0.05	ΔS^\ddagger (J/mol.K) ± 0.1
		35.05	149.6	90.60	-21.7	93.19

Table 2. Langmuir and Freundlich isotherm parameters for the adsorption of MG onto HTC-PN and HTC-APN at 30 °C.

Adsorbent	Langmuir			Freundlich		
	parameters	linear	nonlinear	parameters	linear	nonlinear
HTC-PN	q_{\max} (mg/g)	52.91	52.27	K_F (mg/g) $x(L/mg)^{1/n}$	14.14	18.95
	K_L (L/mg)	0.172	0.204	n	3.38	4.59
	R^2	0.996	0.984	R^2	0.800	0.827
	χ^2	0.0034	6.94	χ^2	0.057	38.18
	SSR	0.0207	41.9	SSR	0.345	229.1
HTC-APN	q_{\max} (mg/g)	97.08	96.18	K_F (mg/g) $x(L/mg)^{1/n}$	23.45	30.98
	K_L (L/mg)	0.306	0.31	n	2.304	3.18
	R^2	0.999	0.994	R^2	0.897	0.920
	χ^2	0.00002	5.20	χ^2	0.058	70.65
	SSR	0.00012	31.2	SSR	0.35	423.9

Table 3. Kinetic model parameters for the adsorption of MG 50 ppm onto HTC-PN and HTC-APN.

Adsorbent	$q_e(\text{exp})$ (mg/g)	Pseudo first order			Pseudo second order		
		q_{\max} (mg/g)	k_1 (min^{-1})	R^2	q_{\max} (mg/g)	k_2 (g/mg.min)	R^2
HTC-PN	26.2	18.45	0.015	0.960	25.00	2.21×10^{-3}	0.994
HTC-APN	28.4	15.59	0.012	0.830	24.15	5.35×10^{-3}	0.990
Adsorbent	Intraparticle diffusion			Liquid film diffusion			
	k_{i1} (k_{i2}) ($\text{mg}\cdot\text{g}^{-1}\cdot\text{min}^{-1/2}$)	I_1 (I_2)	R^2 (R^2)	k_{fd} (min^{-1})	I	R^2	
HTC-PN	1.06 (0.014)	8.95 (0.68)	0.989 (0.999)	0.018	-0.35	0.992	
HTC-APN	0.69 (0.15)	18.80 (24.7)	0.979 (1.00)	0.038	-0.93	0.965	

Table 4. Column kinetic parameters for the adsorption of MG 100 mg/L onto HTC-APN (0.5 g) packed column.

Thomas			Yoon-Nelson			Yan et al		
parameters	linear	non-linear	parameters	linear	non-linear	parameters	linear	non-linear
K_T (mL/min.mg)	0.258	0.23	K_{YN} (min^{-1})	0.0245	0.0219	K_Y (mL/min.mg)	4.25×10^{-5}	4.9×10^{-5}
q_T (mg/g)	37.52	37.92	q_{YN} (mg/g) τ_{YN} (min)	38.11 105.46	38.29 105.95	q_Y (mg/g)	15.05	12.8
R^2	0.977	0.980	R^2	0.9807	0.989	R^2	0.872	0.900
Chi^2	0.049	0.00082	Chi^2	0.055	9.8×10^{-4}	Chi^2	0.36	0.00408
SSR	0.68	0.0116	SSR	0.892	0.0157	SSR	5.85	0.065

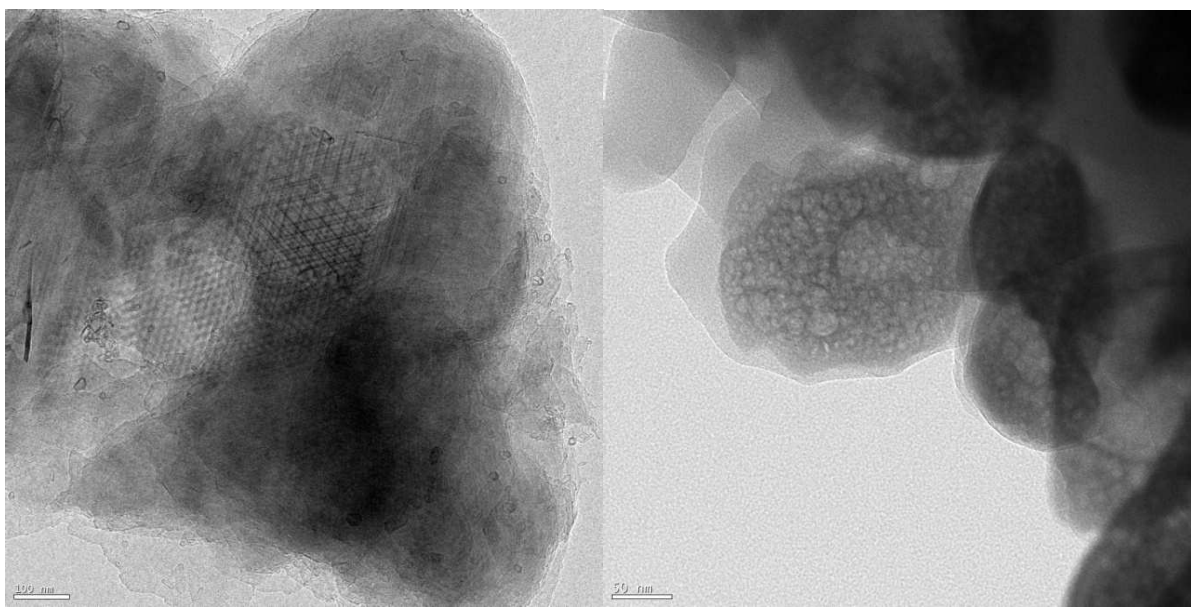


Figure 1. HRTEM images of hydrothermally carbonized pine needle HTC-PN (100 nm) (left) and activated HTC pine needle HTC-APN (50 nm) (right).

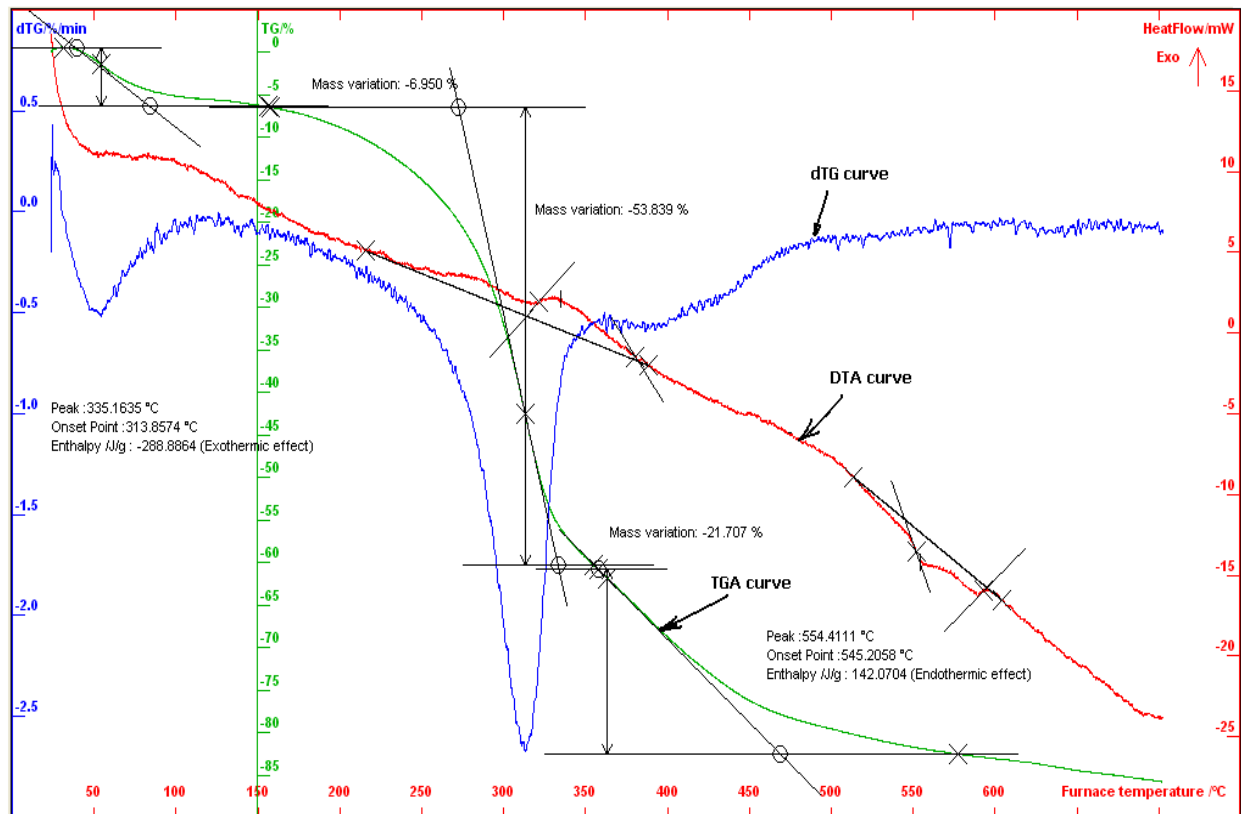


Figure 2. TGA, dTG and DTA curves for Thermal Analysis of HTC-APN.

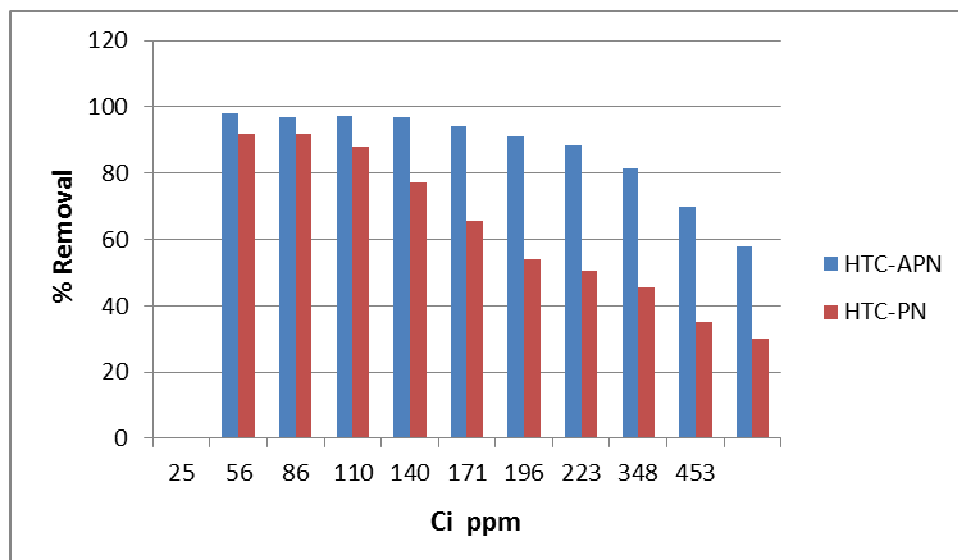


Figure 3. Equilibrium % MG removal depending on initial MG concentration (C_i ppm) for both HTC-PN and HTC-APN for 2g/L adsorbent dose at 30 °C.

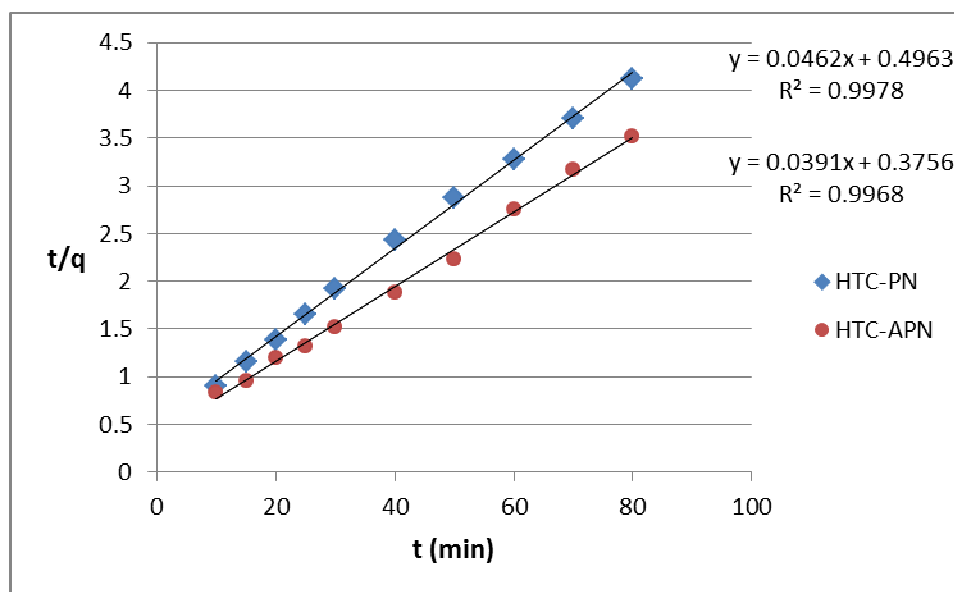


Figure 4. Pseudo-second-order kinetic plot for adsorption of MG (50 ppm) onto HTC-PN and HTC-APN at 30 °C.

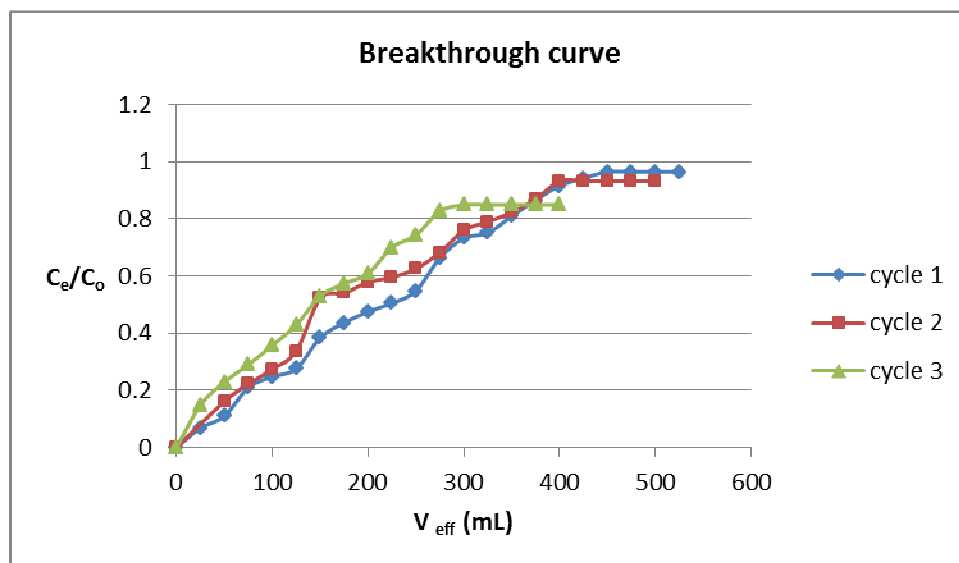


Figure 5. Breakthrough curves for the adsorption of MG (100 mg/L) onto HTC-APN (0.5 g) packed column.

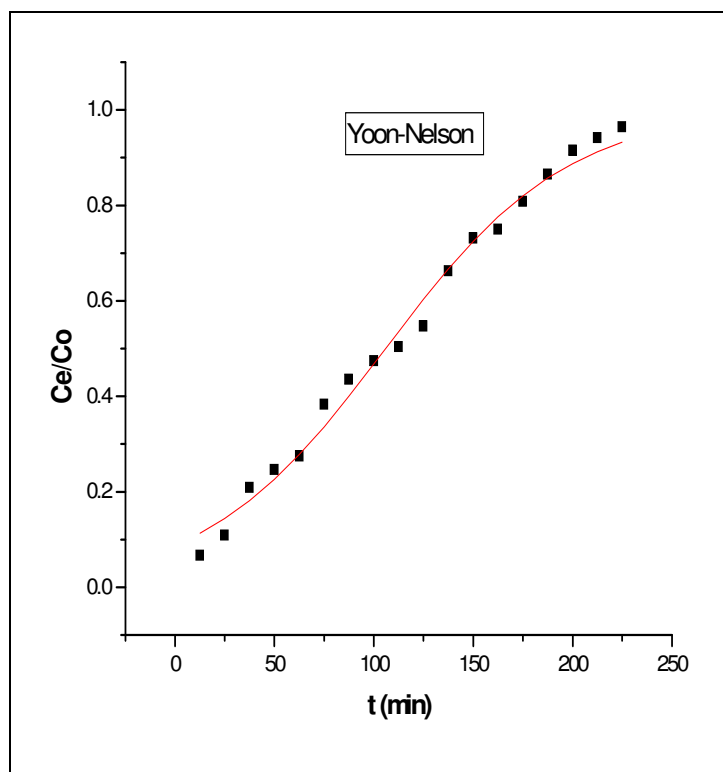


Figure 6. Yoon-Nelson non linear plot for adsorption of MG (100 mg/L) onto column charged with HTC-APN (0.5 g). The points are experimental data, solid line is predicted by Yoon Nelson Model.